Description of Snow Depth Retrieval Algorithm for ADEOS II AMSR

Dr. Alfred Chang and Dr. Richard Kelly
NASA/GSFC

1. Introduction

The development of a snow depth retrieval algorithm for ADEOS II AMSR has been developed from current applications of snow depth retrievals from the Special Sensor Microwave Imager (SSM/I). While the SSM/I is not exactly identical in spatial and waveband configuration to the planned ADEOS II AMSR, it is sufficiently comparable over its four frequencies to be a useful instrument with which to develop a snow retrieval algorithm that is based on the microwave emission properties of snow. The AMSR will have an improved spatial resolution and expanded waveband range compared with the SSM/I and it is expected, therefore, that algorithm development will continue post launch.

2. Underlying principles for snow depth retrieval

There are two aspects to successful snow cover retrieval from space using passive microwave radiometers. First, the snowpack must be detected and second it must be quantified in terms of its snow depth. Fresh of dry snow (containing a negligible amount of liquid water) is a forward scatter of naturally upwelling radiation. Compared with non-snow surfaces, therefore, a snowpack has a distinctive electromagnetic signature at frequencies above 25 GHz. When viewed using passive microwave radiometers from above the snowpack, the scattering of upwelling radiation depresses the brightness temperature of the snow at increasingly high frequencies. This scattering behavior of snow can be exploited to detect the presence of snow on the ground. Having detected the snow, it is then possible to estimate the snow depth of the pack using the degree of scattering. Chang *et al.* (1987) proposed a scheme to estimate the snow depth of a dry, homogeneous, single layer snowpack using radiative transfer theory and the difference between two horizontally-polarized brightness temperature channels at high and low frequencies such that:

$$SD = a \quad DTB) + b \text{ [cm]}, \tag{1}$$

where b is generally regarded as zero and a = 1.59 cm K^1 and the assumption is made that the snow grain radius is 0.3 mm and snow density is 300 kg m^{-3}. The *DTB* term is the difference in brightness temperature between 19 GHz and 37 GHz channels (horizontal polarization). This model works well under the non-complex snow conditions (flat land, no significant forest cover, single layer dry snow) and has been the basis for several SD or snow water equivalent (SWE) retrieval algorithms (e.g. Goodison and Walker, 1994, Foster *et al.*, 1997). However, for global applications there are several additional factors that need to be taken into consideration and incorporated into a retrieval scheme for successful snow depth estimation. These are described in the following section.

3. Confounding factors

Snowpack properties

It is known that at passive microwave wavelengths, shallow snow (less than 10 cm) is transparent to naturally upwelling microwave wavelengths (Armstrong and Brodzik, 1999). This factor can lead to non-detection of the snowpack and hence underestimation of the snow volume. This factor will be most prominent in the early and late parts of the winter season. Use of a high frequency channel (e.g. 89 GHz on AMSR) will assist with this detection although great care must be exerted when using this channel on account of potential atmospheric contamination.

Wet snow can confound snow depth retrievals by depressing the scattering behaviour of the snow. Ultimately, this leads to underestimation of the pack. Unfortunately, at present there is little that can be done to overcome this problem directly although at least the detection of wet snow is possible by using a combination of information about the surface temperature (Sun *et al.*, 1996), polarization difference at 37 GHz (Walker and Goodison, 1994) and immediate snow cover history.

Equation (1) above indicates a static parameterization based on radiative transfer properties of a snowpack (0.3 mm radius grains and 300 Kg m^{-3} density). While this can be applied in some areas around the world at certain times, the nature of snow is such that it can be temporally and spatially dynamic in evolution (Colbeck, 1986). To retain the *a* coefficient in (1) suggests that globally, snow covers are homogeneous in character which clearly is not the case. Although Josberger *et al.* (1995) found that snowpack properties can be homogeneous at regional scales, for continental applications this will not be the case. The *a* coefficient should, therefore, be varied both spatially and temporally and so we have computed a set of coefficients for each month of the year. The spatial distribution of the coefficients is achieved using the seasonal snowpack classification of Sturm *et al.* (1995) which divides the northern hemisphere into 6 dominant regional snow types: taiga, tundra, alpine, maritime, ephemeral and prairie. The *a* coefficients are re-computed for each of these regions based on dominant snowpack characteristics thought to dominate in each region.

False scatterers

Precipitation acts as a confounding effect on snowpack retrievals. This is because precipitation clouds consist of hydrometeors that act like a snowpack on the ground and scatter upwelling microwave radiation away from the radiometer's field of view. Currently it is not possible to detect the presence of snow or retrieve snow depth from beneath precipitating clouds but it is possible to detect precipitation and therefore flag the presence of rainfall. The method used was developed by Grody and Basist (1996).

Forest cover

A major problem in large areas of the globe is the effect that forest cover has on the retrieval of snow depth from passive microwave radiometers (Chang *et al.*, 1996). Dense coniferous (and perhaps deciduous forest at early/late times in the season) depress the microwave scattering signal from snow within the forest causing an under-retrieval of the snow depth. Attempts have been made to overcome the problem (e.g. Foster *et al.*, 1997) but the problem is not easily resolvable at the moment. The Robinson and Kukla (1985) global albedo data set has been used to estimate forest cover through the following relationship:

$$ff = -150albedo + 120 \quad [\%] \qquad (2)$$

where *ff* is the forest fraction in percent and the two coefficients describe a straight line. This linear relationship is based in the fact that for land surfaces that are not water bodies, low albedos (<0.5) are likely to be indicative of dense forest whilst higher albedos (>0.5) are probably indicative of low stand or no vegetation. The range of forest cover is calibrated to between 0 % and 90 %and is then re-scaled linearly to 0 to 1 where 1 represents 100 % and 0 represents 0 % such that the data can be incorporated into (1):

$$SD = a \ DTB) / (1-ff) + b \quad [\text{cm}]. \qquad (3)$$

A full account of this relationship can be found in Foster *et al.* (1997). This relationship is currently under further refinement since the Robinson and Kukla (1985) data set is at 1.0º spatial resolution which is coarser than the scale used in this project (9.28 km equal area grid). In addition, there are better products available and becoming available to provide more up-to date information about the global distribution of forest cover. For example, direct forest cover data are available through the International Geosphere and Biosphere Project (IGBP) (although these are derived from annual average land cover data sets based on the reflective properties of the land surface from AVHRR data). It is expected that in the future, more dynamic forest cover information will be available through MODIS reflectance or land category products that are produced every 16 days. This will provide a better characterization of the forest cover plus it will give improved information about stem volume (rather than percentage cover in a pixel) which is thought to be the key effect on microwave retrievals of snow in forested areas (Kurvonen *et al.*, 1998).

Mountainous terrain

Retrieval of snow depth from complex mountain topography is a challenge for low spatial resolution passive microwave radiometers. This is because within a given footprint in a mountain zone, the variability of snow depth is much greater than in flat terrain. Consequently, to avoid underestimation and overestimation, such

terrain is flagged and avoided in the current version of the algorithm. The GTOPO30 product from the USGS is used to flag mountain topography.

4. Implementation of the algorithm

The algorithm, coded in C, is currently implemented from a Unix Bourne Shell. The procedure is shown by the flow chart in Figure 1 below. The first step is to determine the kind of surface present (flat land, water body on land, ice, ocean, mountainous terrain, snow climatologically (im)possible, forest cover). The climatological possibility of snow cover presence is obtained from Dewey and Heim (1981 and 1983). Unless the surface is flat land without heavy forest cover, the procedure flags the surface type and does not attempt to compute the snow depth. For flat land without heavy forest cover, the algorithm proceeds to Step 2, which reads, in AMSR channel brightness temperatures.

Step 3 determines that the AMSR data are within a reasonable range and that there are no gross data errors in the brightness temperature. Step 4 obtained the surface temperature estimate based global circulation model estimates from the Japanese Meteorological Agency. This step is used to determine whether or not the surface is likely to be too warm and, therefore, the probability is low for the presence of snow. Step 5 screens for precipitation and Step 6 determines whether there is wet or dry snow present and Step 7 estimates the snow depth. If the snow is dry, the algorithm computes the snow depth using equation (3) above. The applied *a* coefficient in (3) dependent on whether or not the underlying soil is dry or wet, the Sturm *et al.* (1995) seasonal snow class and also on the time of year.

5. Validation of algorithm

Two data sets were assembled to validate the algorithm developed for ADEOS II AMSR snow depth estimation. First, a four-year record from 1992 – 1995 of daily GTS meteorological station snow depth measurements and coincident SSM/I brightness temperatures prepared by NASDA, Japan were reanalyzed (see Chang and Koike, 2000). The second data set used was a month of daily global WMO meteorological station snow depth data for January 2001.

1992-1994 data set validation

This data set comprises 86 GTS meteorological stations distributed in the northern hemisphere and quality controlled (originally there were 100 but anomalous and erroneous readings were screened). The data comprise four years of gauged daily snow depth measurements from January 1992 to December 1995. Coincident SSM/I brightness temperatures at each station are also stored in the data set.

Snow depth was estimated using the simple algorithm from equation 1 (hereafter referred to as the "1.59" algorithm) and also using the spatially and temporally dynamic algorithm from equation 3 (hereafter referred to as the Chang algorithm). The estimated snow depths from both algorithms were compared with the gauge data and the mean absolute error (an indicator of the magnitude of algorithm error) and the mean error (a measure of algorithm bias) for both algorithms for the entire four-year period was computed. Figure 1 shows two histograms of the results. The mean absolute error (MAE) histogram shows that both algorithms perform similarly well at the global scale. The average MAE for the Chang algorithm is 16.6 cm while for the "1.59" algorithm it is 16.1 cm. This would suggest that the errors are similar in magnitude for each station over the four years. However, inspection of the bias in the adjacent histogram demonstrates that the Chang algorithm bias is much closer to 0 cm than the "1.59" algorithm (-5.9 cm and –0.3 cm for Chang and "1.59" respectively). This suggests that although the absolute errors are similar, the underestimation of snow depth traditionally found in the passive microwave estimates, is reduced in the new algorithm. The reason for this could be on account of the fact that the new Chang algorithm incorporates the "forest effect" in its estimates thus reducing the bias (underestimation) commonly found in retrievals. Figure 2 shows the MAE and ME for sites where the forest fraction is greater than 30%. Again a similar situation emerges with similar average MAE estimates for both algorithms (19.6 cm and 21.3 cm for the "1.59" and Chang algorithms respectively). However, the average bias in the Chang algorithm is much less under high forest fractions with an average ME of –13.7 cm and 1.3 cm for the "1.59" and Chang algorithm respectively.

Figure 1
AMSR Snow depth algorithm logic

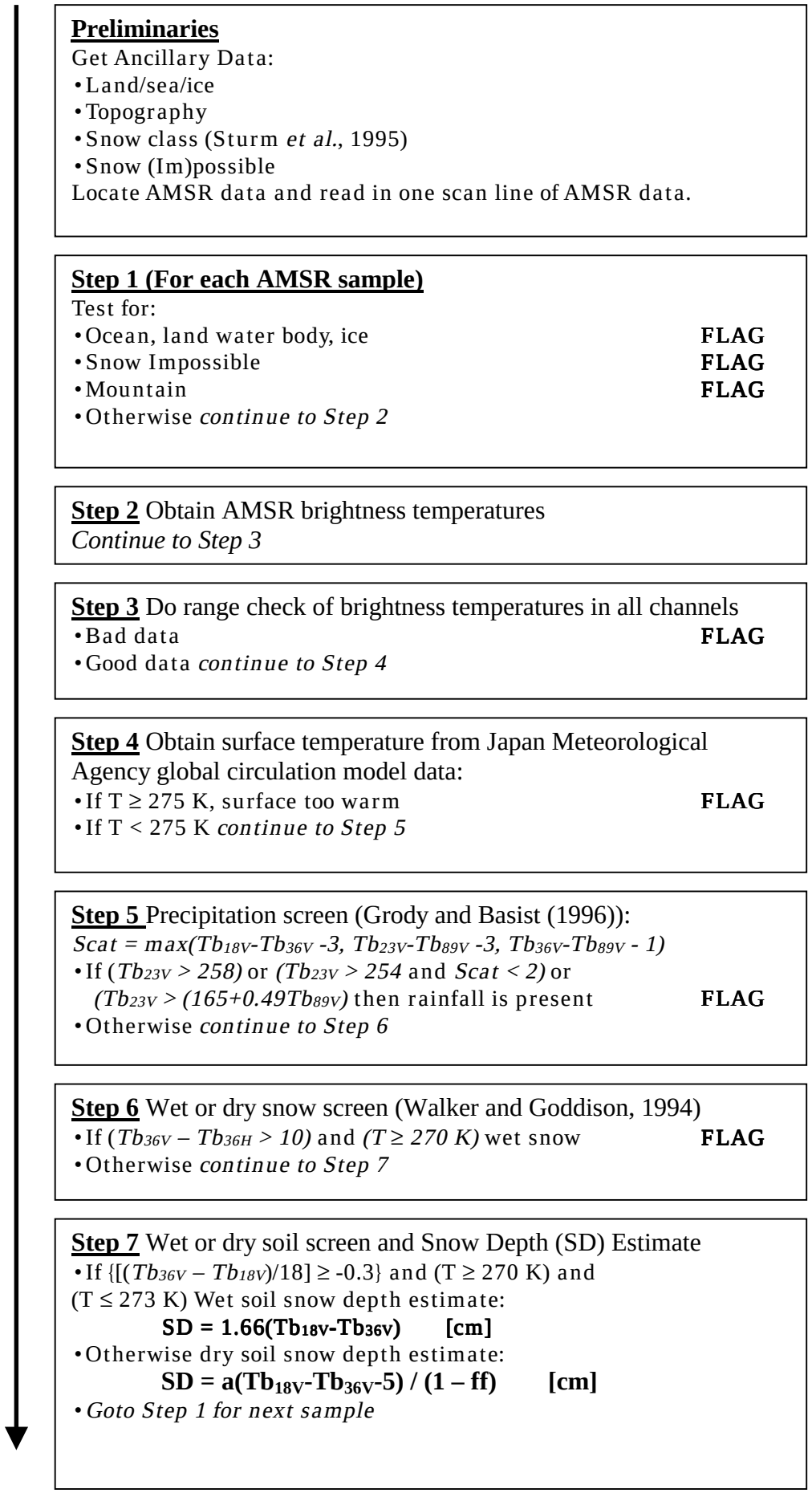

January 2001 data set validation

A similar exercise was conducted for a relatively constrained (temporally) data set but which contained many more gauged snow depth measurements. Data were obtained from the WMO's network of approximately 600 stations (many in the GTS network) in the northern hemisphere. MAE and ME calculations were made at four distinct spatial scales to determine whether the Chang and "1.59" algorithms might perform differently. Computations were made at a global scale, North America data, Canadian data and Northern Great Plains data. The results are shown in the time plots in Figure 3. It is clear that the MAE values are, again, similar for both the "1.59" and Chang algorithms. However, the bias in the Chang algorithm is reduced significantly in the Chang algorithm estimates. This is the case at all spatial scales with the anomalous exception of the ME for the Northern Great Plains where the "1.59" algorithm does marginally better.

Again, it was suggested that the reason for the improved bias revealed in the Chang results is due to the fact that the forest effect is incorporated in the algorithm. Figure 4 is similar to Figure 3 except that again, computations of MAE and ME were performed only for pixels with forest fraction greater than 30%. The results support the argument that the Chang algorithm does reduce the overall bias in the estimates caused by forest cover.

Figure 5 Shows visually representation of the two algorithms for 1 January 2001. The left panel is the result of applying the "1.59" algorithm and the right panel is a representation of the Chang algorithm. The same screens (rainfall, mountains etc.) are applied in both algorithms so that the differences between the two retrievals are the spatial variation in snow depth.

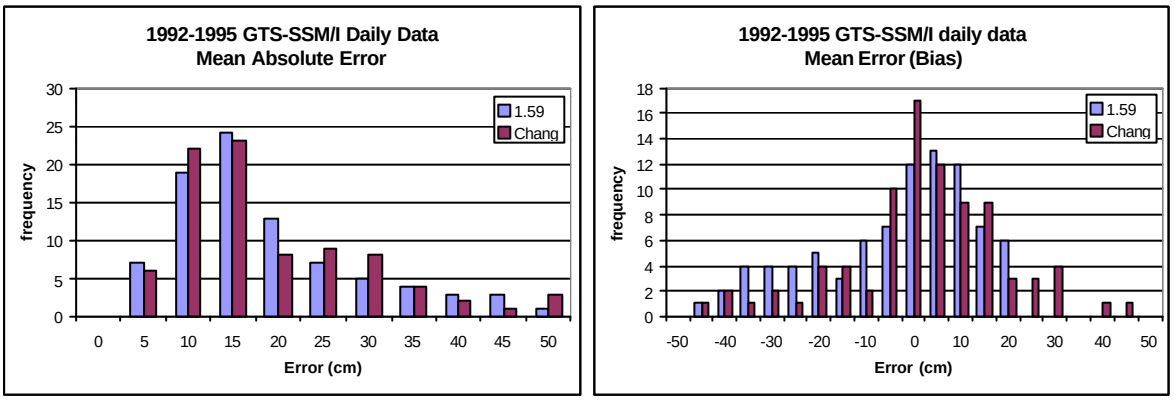

Figure 1. Global validation (mean absolute error and bias) of AMSR (chang) algorithm compared with standard 'static' algorithm (see equation 1) for 86 global GTS snow depth gauge stations.

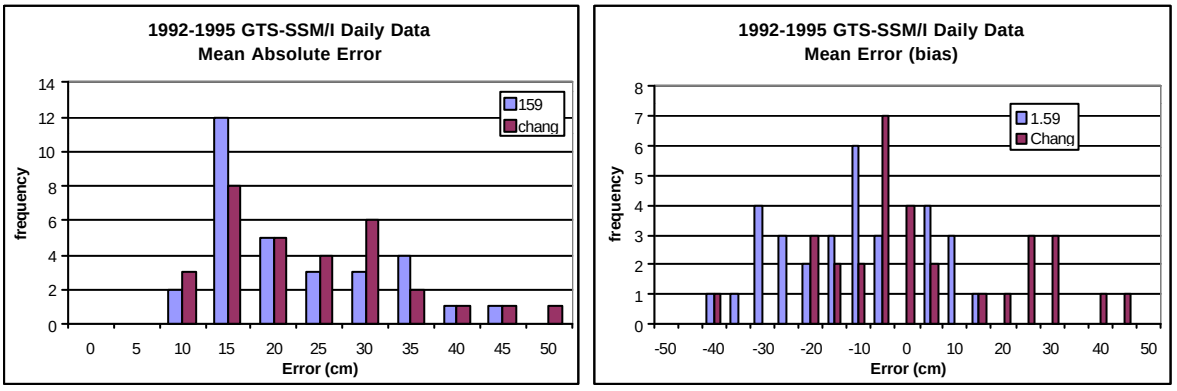

Figure 2. Global validation (mean absolute error and bias) of AMSR (chang) algorithm compared with standard 'static 1.59' algorithm (see equation 1) for 86 global GTS snow depth gauge stations where forest fraction is greater than 30%.

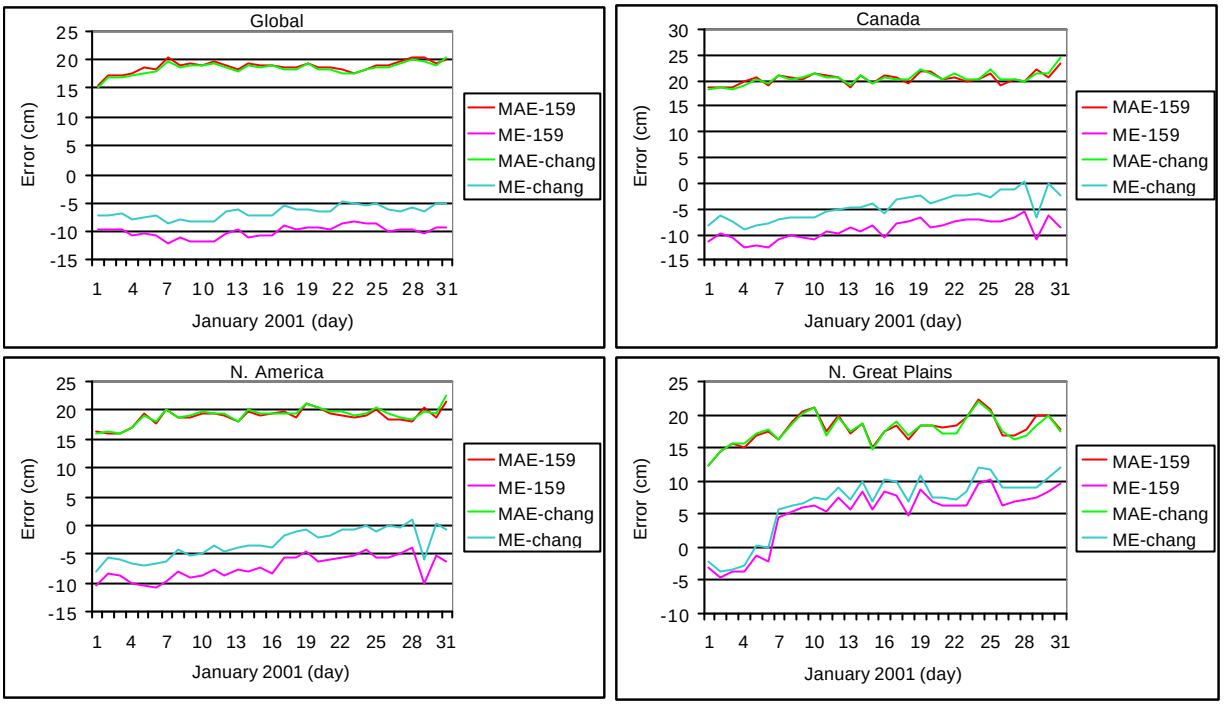

Figure 3. Comparison of 'Chang' and '1.59' snow depth algorithm validation. MAE is the mean absolute error and ME is the mean error (bias). The comparison is for applications of the algorithms in January 2001 and from all stations at global, North America, Canada and Northern Great Plains scales.

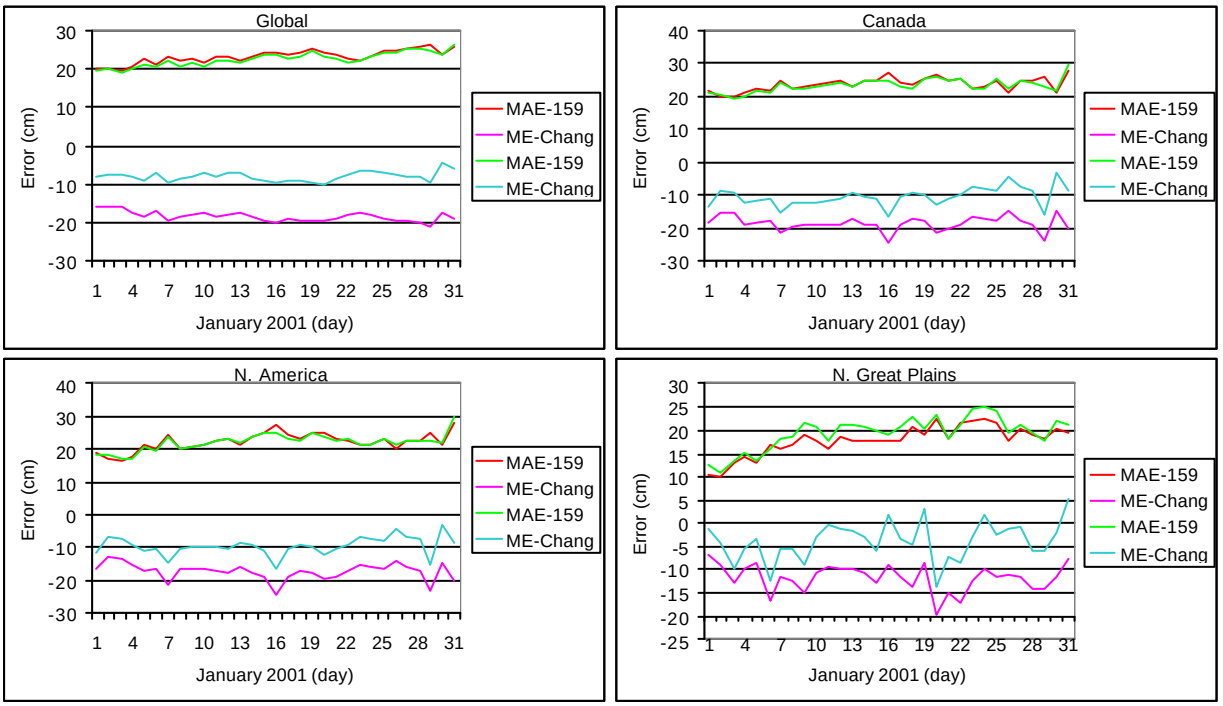

Figure 4. Comparison of 'Chang' and '1.59' snow depth algorithm validation. MAE is the mean absolute error and ME is the mean error (bias). The comparison is for applications of the algorithms in January 2001 for EASE grid pixels that are characterized with forest cover greater than 30% and from all stations at global, North America, Canada and Northern Great Plains scales.

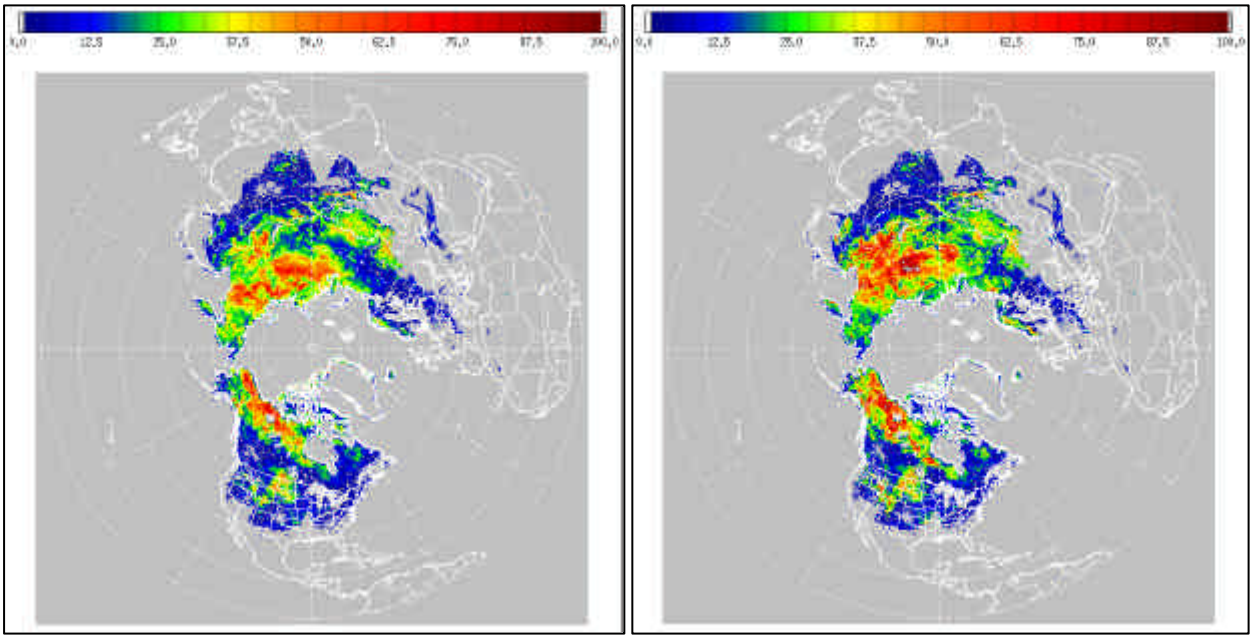

Figure 5. Visualisation of the "1.59" snow depth algorithm (left) and the Chang snow depth algorithm (right) for 1 January 2001. The colour scale units are in cm.

6. Future developments

Results from the work to date are very encouraging and suggests that the new algorithm development should improve the old static coefficient methodology described by equation 1. However, the retrieval residuals or errors still need further constraint. Despite a retrieved error (MAE) of 16.6 cm globally, translating this into a SWE produces a value of 1.6 mm for fresh snow (with a density of 100 kg m^{-3}) and more for seasonal snow with higher density. It is clear, however, that the spatial distribution of the coefficient *a* in equation 3 is important for successful snow depth retrievals. While the Sturm *et al.* (1995) seasonal snow classification is undoubtedly an invaluable global descriptor that can help, newer, more sensitive descriptors are needed that can provide higher spatial resolution for coefficient spatial extrapolation. This is one area that we are currently developing using geostatistics and land cover data sets and results to date are promising (with further reduced ME and reduced MAE values). In addition, it is clear that successful estimation of daily local snow depth variability will benefit from a dynamic temporal component that could be included in the algorithm to determine variations in snowpack properties. While problematic, this aspect is the subject of current development activities.

An important future development that will assist with the algorithm validation and development is our participation in the Cold Land Processes Field Experiment (CLPX) in North American planned for the 2002-2003 winter season in Colorado. This experiment is part of the NASA Global Water and Energy Cycle (GEWEC) initiative, the Global Energy and Water Cycle Experiment (GEWEX) and the GEWEX Americas Prediction Project (GAPP). The broad objectives of the CLPX are to develop our understanding of cold land processes by increasing our ability to characterize the spatial and temporal variability of snow, ice and frozen ground in the natural environment, and to identify and quantify the various uncertainties associated with remote sensing observations and models of cold land processes, thereby improving our abilities to predict the behavior of various cold land processes (NASA, 2001). As part of this, a significant number of field experiments are planned for February and March 2002 and 2003 to measure snowpack parameters intensively in three 25 km x 25 km and 1 km x 1 km cells in Colorado. The measurement suite will include snow depth, SWE, and surface wetness and roughness and various snow descriptors obtained from snow pits. It is planned that this experiment will also have access to ground-based and airborne radiometers plus a suite of satellite observations. The aircraft flight lines will cover several the AMSR foot-prints (25 km x 25 km). Consequently, it is anticipated that several of the outstanding uncertainties associated with snow depth and SWE retrieval form microwave radiometry will be

addressed. This information will assist directly with out efforts for the development of ADEOS II AMSR snow depth retrieval algorithm.

References

Armstrong, R.L. and M.J. Brodzik, (1999) A twenty year record of global snow cover fluctuations derived from passive microwave remote sensing data, *5th Conference on Polar Meteorology and Oceanography*, American Meteorological Society. Dallas, TX, 113-117.

Chang, A.T.C., J.L. Foster and D.K. Hall, (1987) Nimbus-7 derived global snow cover parameters, *Annals of Glaciology*, 9, 39-44.

Chang, A.T.C., J.L. Foster and D.K. Hall, (1996) Effects of forest on the snow parameters derived from microwave measurements during the BOREAS winter field experiment. *Hydrological Processes*, **10**: 1565-1574.

Chang, A.T.C. and T. Koike (2000) Progress in AMSR snow algorithm development, in Pampaloni, P. and S. Paloscia (Eds), Microwave Radiometry and Remote Sensing of the Earth's Surface and Atmosphere, VSP, p515-523.

Colbeck, S.C. 1986 Classification of seasonal snow cover crystals, *Water Resources Research*, **22(29)**: 59S-70S.

Dewey, K.F. and R.Heim, Jr. (1981) Satellite observations of variation in Northern Hemisphere seasonal snow cover, NOAA Technical Report NESS 87, 83 pp.

Dewey K.F. and R. Heim, Jr. (1983) Satellite observations of variations in Southern Hemisphere snow cover, NOAA Technical Report NESDIS 1, 20 pp.

Foster, J.L, A.T.C. Chang and D.K. Hall, (1997) Comparison of snow mass estimates from a prototype passive microwave snow algorithm, a revised algorithm and snow depth climatology, *Remote Sensing of Environment*, **62**: 132-142.

Goodison, B. and A. Walker, (1994) Canadian development and use of snow cover information from passive microwave satellite data, In Choudhury, B., Kerr, Y., Njoku, E., and Pampaloni, P. (eds) *Passive Microwave Remote Sensing of Land-Atmosphere Interactions*, Utrecht: VSP BV, 245-62.

Grody, N.C. and A.N. Basist (1996) Global identification of snowcover using SSM/I measurements, *IEEE Transactions on Geoscience and Remote Sensing*, **34(1)**: 237-249.

Josberger, E., P. Gloersen, A. Chang and A. Rango, (1995) Snowpack grain size variations in the upper Colorado River basin for 1984-1992. *Journal of Geophysical Research*, 101, 6679-6688.

Kurvonen, L., J. Pulliainen, M. Hallikainen (1998) Monitoring of boreal forests with multitemporal special sensor microwave imager data, *Radio Science*, **33(3)**: 731-744.

NASA, (2001) NASA Cold Land Proccesses Field Experiment Plan 2002-2004, Cold Land Processes Working Group, NASA/ESE/LSHP, http://lshp.gsfc.nasa.gov.

Robinson, D.A. and G. Kukla, (1985) Maximum surface albedo of seasonally snow covered lands in the Northern Hemisphere. *Journal of Climate and Applied Meteorology* **24**: 402-411.

Sturm, M., J. Holmgren and G.E. Liston, (1995): A seasonal snow cover classification system for local to global applications. *Journal of Climate*, **8**, 1261-1283.

Sun, C.Y, C.M.U. Neale and J.J. McDonnell, (1996): Snow wetness estimates of vegetated terrain from satellite passive microwave data. *Hydrological Processes*, **10:** 1619-1628.

Walker, A., and B. Goodison, (1993) Discrimination of a wet snow cover using passive microwave satellite data, *Annals of Glaciology*, **17**: 307-311.